

## Extrusion of Aluminum Alloys Prepared from Mechanically Alloyed Powder

\*R. E. Coelho, \* S. J. G. de Lima and \*\*F. Ambrozio

\*Universidade Federal da Paraíba CT/DTM-LSR CEP: 58059-900 - João Pessoa, PB-Brasil

\*\*Ipen- Instituto de Pesquisas Energéticas e Nucleares  
Cidade Universitária-Travessa R, 400 CEP: 05508-900 - São Paulo, SP - Brasil

\* [roesco@funape.ufpb.br](mailto:roesco@funape.ufpb.br)

\* [jackson@lsr.ct.ufpb.br](mailto:jackson@lsr.ct.ufpb.br)

\*\* [fambrosi@net.ipen.br](mailto:fambrosi@net.ipen.br)

**Keywords:** Aluminum alloy, mechanical alloying, indirect extrusion.

**Abstract.** Aluminum alloys were produced by means of mechanical alloying and subsequently hot extrusion, microstructure were studied and their properties determined. Two Al-Fe-X-Si (X=V or Nb) compositions,  $Al_{90.8}-Fe_{6.2}-Nb_{1.0}-Si_{2.0}$  and  $Al_{90.8}-Fe_{6.2}-V_{1.0}-Si_{2.0}$  (at. %), were prepared by mechanical alloying from the respective metallic powders. The powder mixtures and extruded materials were characterized by X-ray diffraction, differential scanning calorimetry, scanning (SEM) and transmission (TEM) electron microscopy, and energy dispersive spectrometry (EDS). Extruded materials were also characterized for hardness and tensile strength.

### Introduction

Powder metallurgy process (PM) using mechanical alloying technique (MA) is able to produce a material with a superior strength [1]. The solid interaction by MA has attracted a large amount of study [1-4]. Mechanical alloying method has been recognized as a complex process, which can be applied to the processing of advanced materials at low cost. In general, both stable and metastable phases can be produced by mechanical alloying [4]. MA takes place under high energy milling balls agitation, resulting in cold welding and fracturing of the metallic powder mixture, and some non-metallic powders can also be added [5]. The mechanisms of the state reactions during high-energy milling have been intensively studied. This technique permits obtaining an alloy by the means of a mechanical processing, completely in solid-state, for subsequent consolidation [5,6]. The nano-structures produced by mechanical attrition are not caused by cluster assembling, but by the structural decomposition of coarser-grained structures, as the result of severe plastic deformation. The thermal stability of nanocrystalline microstructure is of major importance both for hot consolidation of the powders and for any possible elevated temperature applications. Mechanical alloying offers many advantages over the processes used for conventional aluminum alloys, including alloying with a fine microstructure and a high-volume fraction of thermal stable dispersoids. Al-Fe-Mn alloys and some rare earth elements produced by MA are presented for high-temperature applications. Mechanically alloyed (MA) aluminum alloys such as AlFeMn [7], AlTiNb [8], AlMnCe [9] and the other binary and ternary alloys have been studied but there are only a few papers on MA Al-Fe-V-Si alloys [10].

This paper presents the microstructure and properties of MA alloys by milling of elemental powders of Al, Fe, X, and Si, (X= V or Nb) followed by vacuum hot pressing and hot extrusion.

### Experimental

Two Al-Fe-X-Si (X=V or Nb) compositions,  $Al_{90.8}-Fe_{6.2}-Nb_{1.0}-Si_{2.0}$  and  $Al_{90.8}-Fe_{6.2}-V_{1.0}-Si_{2.0}$  (at. %), were prepared by mechanical alloying from the respective metallic powders. The mean particle sizes of the starting elemental powders were: Al-50 $\mu$ m, Fe-100 $\mu$ m, Nb-100 $\mu$ m, V-1mm size flakes and Si-100 $\mu$ m. Preliminarily, powder mixture for composition  $Al_{90.8}-Fe_{6.2}-Nb_{1.0}-Si_{2.0}$

milling experiments were conducted for 5, 10, 20, and 40 hours only at 1400 rpm to observe the powders morphology evolution and possible new phase formation. The powder mixture,  $\text{Al}_{90.8}\text{-Fe}_{6.2}\text{-Nb}_{1.0}\text{-Si}_{2.0}$  composition was also attrition milled for 10 hours at 800 rpm. The  $\text{Al}_{90.8}\text{-Fe}_{6.2}\text{-V}_{1.0}\text{-Si}_{2.0}$  (at. %) composition was attrition milled at 800 and 1400 rpm for 10 hours. Additionally the  $\text{Al}_{90.8}\text{-Fe}_{6.2}\text{-V}_{1.0}\text{-Si}_{2.0}$  (at. %) composition was also attrition milled for 5 hours at 1400 rpm, and for 20 hours at 800 rpm.

The powders were mechanically alloyed in an attritor mill with a vertical shaft in a jar under a protective nitrogen atmosphere. The milling vial of the alloy was made of polyethylene with 81mm in diameter. The balls were made of chrome steel with 7mm in diameter.

After milling, the powders were removed in air atmosphere and vacuum hot pressed ( $6 \times 10^{-3}$  torr) under a pressure of 530MPa and a temperature at 340°C. The compacted billet of 31mm in diameter by 30mm in length was hot at 500°C and extruded in a laboratory extrusion machine by indirect extrusion. Indirect extrusion was done with an extrusion ratio of 6:1. Hand-mixed composition (0hour) was also vacuum hot pressed and extruded, and subsequently used as reference materials.

The morphology evolution of the MA powders in the  $\text{Al}_{90.8}\text{-Fe}_{6.2}\text{-Nb}_{1.0}\text{-Si}_{2.0}$  composition were examined in a scanning electron microscope (SEM) and samples of the extruded bars in the two compositions were examined in a transmission electron microscope (TEM). TEM specimens were of 3mm disks approximately and 200 $\mu\text{m}$  in thickness. The center of these discs was thinned to approximately 300nm by double electrolytic jet polishing in Tenupol 3 (at 25V and 300mA) with a 10% perchloric acid 90% methanol solution at minus 10°C.

X-ray diffraction measurements were carried out in a Rigaku diffractometer with  $\text{CuK}\alpha$  radiation. The morphology of the powders was observed in a Leo Steroscan 440 SEM and a Philips CM 200 TEM containing a lithium/ silicon X-ray detector. The DSC experiments were performed in a Shimadzu DSC 50, under dynamic nitrogen atmosphere with 5°C/min of heating.

Tensile tests were carried out at room temperature, of 200 and 350°C. Vickers hardness measurements were performed on extruded bars at room temperature and a load of 0.98N. An Instron 4400R universal testing machine with a load cell of 5kN and at 1.67 $\times 10^{-3}$ mm/s was used in the tensile tests.

## Results and discussion

The shapes of the powder particles  $\text{Al}_{90.8}\text{-Fe}_{6.2}\text{-Nb}_{1.0}\text{-Si}_{2.0}$  after 5, 10, 20 and 40 hours of milling at 1400rpm are shown in Fig. 1. The powder milled for 5 hours at 1400rpm, had the flake morphology, this time there was predominance of welding. At 1400rpm after 10 hours, the powder particles are more round and smaller, and welding prevailed over fracture.

Fig. 2 shows the X-ray diffractogram (XRD) of the powder particles  $\text{Al}_{90.8}\text{-Fe}_{6.2}\text{-Nb}_{1.0}\text{-Si}_{2.0}$  after 1, 5, 10, 20 and 40 hours. In the powder that was MA for 1 hour and 5 hours at 1400 rpm respectively, no new phase was detected by X-ray diffraction. This pattern showed peaks corresponding to the elements Al, Fe, Nb and Si. After 10 hours of milling,  $\text{AlNb}_2$  phase was formed. There were no other phases during milling. The decrease of intensity and enlargement of the diffraction peaks during the milling time is noted. This could be due to the increase in number of defects in the elemental powders.

Fig. 3 shows the (XRD) of the extruded materials  $\text{Al}_{90.8}\text{-Fe}_{6.2}\text{-V}_{1.0}\text{-Si}_{2.0}$  during 5 and 10 hours of milling at 1400rpm, during 10 and 20 hours at 800rpm and extruded materials  $\text{Al}_{90.8}\text{-Fe}_{6.2}\text{-Nb}_{1.0}\text{-Si}_{2.0}$  during 10 hours of milling at 800 and 1400rpm.

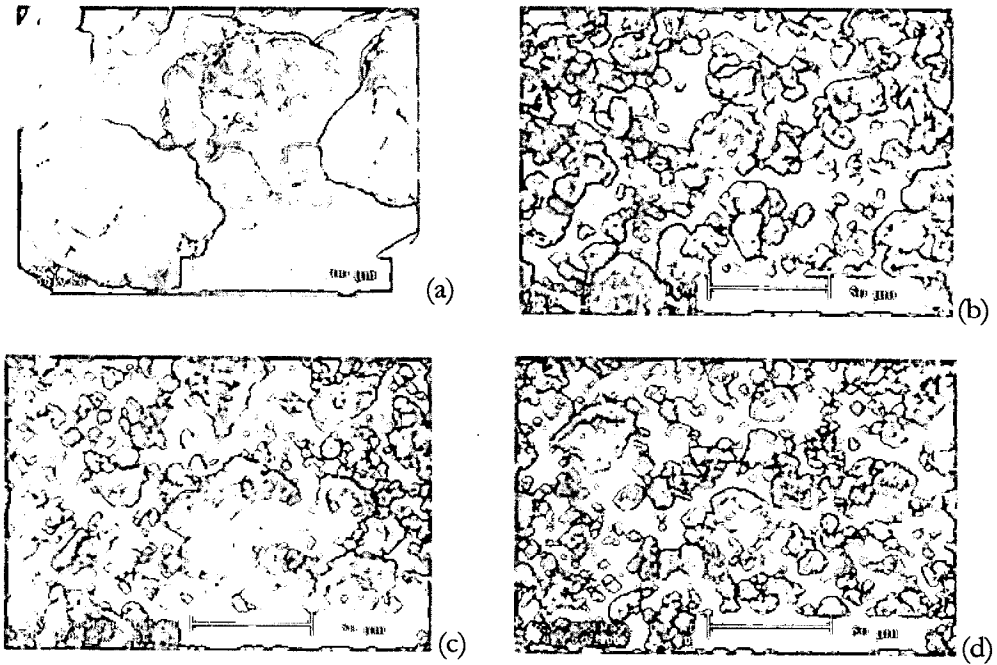


Fig. 1: Morphology of powder particles after (a)5, (b)10, (c)20 and (d)40 hours of milling at 1400 rpm.

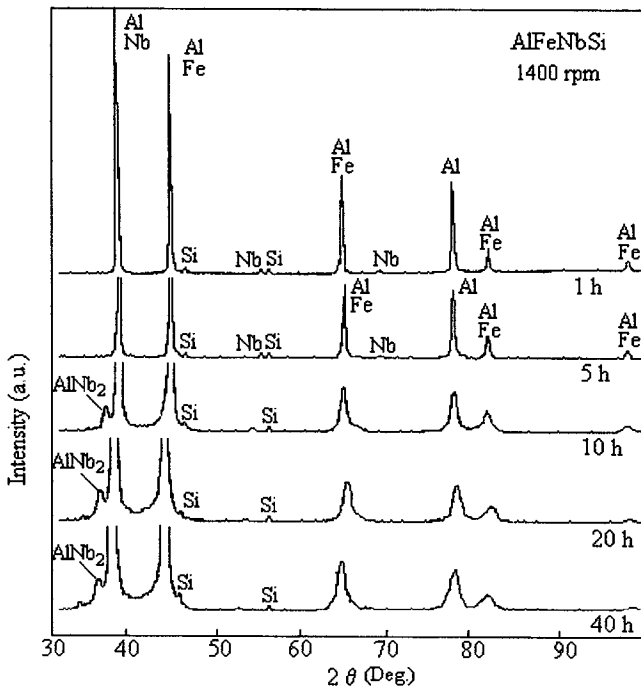


Fig. 2: XRD of mechanically alloyed AlFeNbSi powder after 1, 5, 10, 20 and 40 hours at 1400rpm.

In the bar extruded from  $\text{Al}_{90.8}\text{-Fe}_{6.2}\text{-X}_{1.0}\text{-Si}_{2.0}$  ( $\text{X} = \text{Nb}$  or  $\text{V}$ ) powder for 10h at 800rpm, the hexagonal  $\text{Al}_8\text{Fe}_2\text{Si}$  phase, with cell parameters  $a=1.243\text{nm}$  and  $c=2.626\text{nm}$  was found (Fig. 3a,b). In the same pattern, the Si peak disappeared and reaction of this element to form the hexagonal phase.

In the bar extruded from  $\text{Al}_{90.8}\text{-Fe}_{6.2}\text{-X}_{1.0}\text{-Si}_{2.0}$  ( $\text{X} = \text{Nb}$  or  $\text{V}$ ) powder for 5 and 10h at 1400 rpm, cubic phase  $\alpha\text{-Al}_{12}(\text{Fe},\text{X})_3\text{Si}$  was identified. This quaternary alloy has been obtained by rapid solidification [11-13] and is based on crystallographic studies carried out by Cooper on ternary alloys  $\alpha\text{-(AlMnSi)}$  and  $\alpha\text{-(AlFeSi)}$  [14,15].

It can be observed in the XRD of the  $\text{Al}_{90.8}\text{-Fe}_{6.2}\text{-Nb}_{1.0}\text{-Si}_{2.0}$  material, the  $\text{AlNb}_2$  phase remained in steady state. The intermetallic phase  $\text{AlNb}_2$  present cell parameter  $a=0.997\text{nm}$  and  $c=0.517\text{nm}$ .

It is important to note, the extruded bar from MA powder for 10 hours of milling at 800rpm from two composition, the formation phase is  $\text{Al}_8\text{Fe}_2\text{Si}$ . The increased rotation of the mill and the same time (10 hours) of process have influenced for the formation of an  $\alpha\text{-Al}_{12}(\text{Fe},\text{X})_3\text{Si}$  phase.

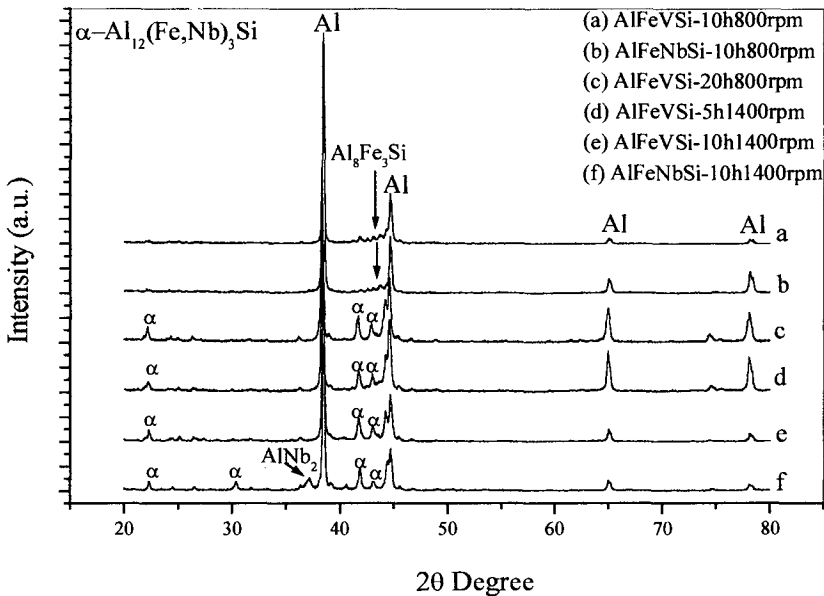


Fig. 3: XRD of the extruded bar, (a) AlFeVSi-10h at 800rpm, (b) AlFeNbSi-10h at 800rpm, (c) AlFeVSi-20h at 800rpm (d) AlFeVSi-5h at 1400rpm (e) AlFeVSi-10h at 1400rpm (f) AlFeNbSi-10h at 1400rpm.

Fig. 4a shows the transmission electron micrograph of  $\text{Al}_8\text{Fe}_2\text{Si}$  phase in the extruded bar of the alloy milled for 10h at 800rpm. This phase is irregular and nearly spherical with diameter of approximately 500nm.

Fig. 4b shows the  $\alpha\text{-Al}_{12}(\text{Fe},\text{V})_3\text{Si}$  phase in the transmission electron micrograph of the extruded bar of the alloy milled 10h at 1400rpm. This phase also has a nearly spherical form, with diameter in the range of 50 to 100nm. Microanalysis of this phase by EDS in the TEM presented the composition of  $\text{Al}_{77.29}\text{Fe}_{10.53}\text{V}_{5.23}\text{Si}_{6.95}$  (at%). This represents only an approximate composition of the quaternary  $\alpha\text{-Al}_{12}(\text{Fe},\text{V})_3\text{Si}$  phase.

Fig. 4c shows the  $\text{AlNb}_2$  and the  $\alpha\text{-Al}_{12}(\text{Fe},\text{Nb})_3\text{Si}$  phase in the transmission electron micrograph, of the extruded bar of the alloy milled for 10h at 1400rpm. The  $\text{AlNb}_2$  phase has a nearly polygonal morphology, with diameter in the range of 50 to 65nm and  $\alpha\text{-Al}_{12}(\text{Fe},\text{Nb})_3\text{Si}$  phase has a nearly spherical form, with diameter in the range of 20 to 40nm. Microanalysis of this phase by EDS in the TEM presented the  $\text{Al}_{77.95}\text{Fe}_{13.55}\text{Nb}_{2.97}\text{Si}_{5.53}$  (at%) composition. This represents only an approximate composition of the quaternary  $\alpha\text{-Al}_{12}(\text{Fe},\text{Nb})_3\text{Si}$  phase.

The formation of the intermetallic  $\alpha\text{-Al}_{12}(\text{Fe},\text{X})_3\text{Si}$  phases observed in extruded bars takes place during heating of the milled powder for pressing and extrusion. Formation of the  $\alpha\text{-Al}_{12}(\text{Fe},\text{V})_3\text{Si}$  phase in powder heated after mechanical alloying has been reported [10].

Vickers microhardness ( $\text{HV}_{100}$ ) at room temperature, yield strength, tensile strength and elongation of the extruded bars at room temperature are presented in Table 1. The value of the Vickers microhardness is the mean of 12 determinations. The yield strength, tensile strength and elongation values have the means values of three determinations and samples from different extrusions.

Fig. 5 shows the ultimate tensile strength measured as a function of test temperatures of the extruded bar of the  $\text{AlFeXS}$  ( $\text{X}=\text{V}$  or  $\text{Nb}$ ) alloy processed with MA powders milled for 10h at 800 and 1400rpm. It can be observed, in the figure, that the UTS of the  $\text{AlFeXS}$  alloy decrease, with the increase rotation of milling.

The  $\text{AlFeXS}$  alloys have a typical ductility. At room temperature, elongation is 5.8%. It decreases, with increasing temperature. At  $200^\circ\text{C}$ , elongation is 3.4% and at  $350^\circ\text{C}$ , it is 3.0%. The mechanical properties of the material are probably due to the nanometric size precipitates of the  $\text{Al}_{12}(\text{Fe},\text{V})_3\text{Si}$  phase.

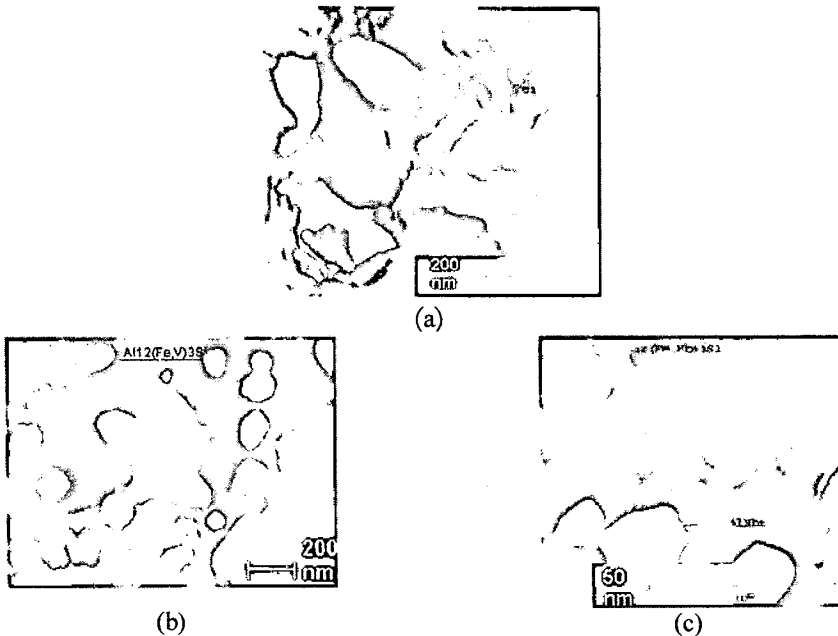


Fig. 4: TEM bright-field micrographs showing: (a) extruded material from powder for 10h at 800rpm consisting of  $\text{Al}_8\text{Fe}_2\text{Si}$  phase and  $\alpha\text{-Al}$ , (b, c) extruded material from powder for 10h at 1400rpm consisting of  $\alpha\text{-Al}_{12}(\text{Fe},\text{X})_3\text{Si}$  ( $\text{X}=\text{V}$  or  $\text{Nb}$ ) and  $\alpha\text{-Al}$ .

Table1: Mechanical properties of extruded bars at room temperature.

| Material               | HV <sub>100</sub><br>(kgf/mm <sup>2</sup> ) | UTS<br>(MPa) | YS<br>(MPa) | Elong.<br>(%) |
|------------------------|---|--------------|-------------|---------------|
| AlFeNbSi (0 h)         | 32 (±6)                                     | 145(±14)     | 135         | 12.5          |
| AlFeNbSi (5h 800rpm)   | 50 (±5)                                     | 196(±12)     | 169         | 11.5          |
| AlFeNbSi (10h 800rpm)  | 115 (±3)                                    | 337(±8)      | 286         | 5.3           |
| AlFeNbSi (10h 1400rpm) | 215 (±3)                                    | 547(±11)     | 497         | 5.1           |
| AlFeVSi (10h 800rpm)   | 114 (±4)                                    | 316(±9)      | 262         | 6.2           |
| AlFeVSi (5h 1400rpm)   | 145 (±4)                                    | 364(±12)     | 332         | 6.0           |
| AlFeVSi (20h 800rpm)   | 183 (±5)                                    | 507(±10)     | 421         | 5.8           |
| AlFeVSi (10h 1400rpm)  | 209 (±4)                                    | 524(±10)     | 478         | 5.8           |

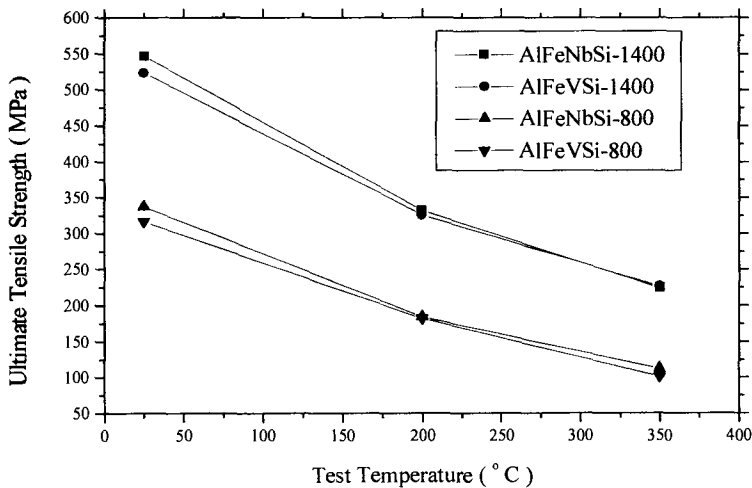


Fig. 5: UTS measured as a function of testing temperatures of the AlFeXSi.

## Conclusions

The addition of control agents [1] like stearic acid, methanol or polyethylene based wax are not necessary when the milling is performed in a polyethylene jar.

The AlNb<sub>2</sub> phase was detected in the mechanical alloying powder and the cubic  $\alpha$ -Al<sub>12</sub>(Fe,X)<sub>3</sub>Si phase was detected only after extrusion of the mechanical alloying powders, due to the reaction between the elements during heating of the alloy.

The ultimate tensile strength, higher in the extruded material from powder milling for 10h at 1400rpm, can be attributed to the process of mechanical alloying that contributed to the formation of the cubic  $\alpha$ -Al<sub>12</sub>(Fe,X)<sub>3</sub>Si phase.

## Acknowledgements

The authors wish to thank CNPq for the financial support of this project.

**References**

- [1] J. S. Benjamin, M. J. Bomford, *Metall. Trans.* 8A (1977) p.1301.
- [2] X. P. Niu, P. Le Brun, L. Froyen, C. Peytour and L. Delaey, *Adv. Powder Metall. & Part. Mater.* 7 (1992), p.271.
- [3] C. C. Koch, *Mater. Trans., JIM.* 36 [2] (1995), p.85.
- [4] R. B. Schwarz, *Scr. Metall. Mater.* 34 [1] (1996), p.37.
- [5] G.J. Fan, X.P Song, M.X. Quan and Z.Q. Hu, *Mater. Sci. Eng.* A231 (1997), p.112.
- [6] B. S. Murty, S. Ranganathan, *Int. Mat. Rev.* 43 [3] (1998), p.101.
- [7] X. Niu, P. Brun, L. Froyen, C. Peytour, L. Delaey, *Powder Metall. Int.* 25 [3] (1993), p.118.
- [8] D. C. Jia, Y. Zhou, T. C. Lei, *Mater. Sci. Eng.* A232 (1997), p.183.
- [9] Yu Ji, Marke Kallio, Tuomo Tiainen, *Scr. Mater.* 42 (2000), p.1017.
- [10] L. J Zheng, J. X. Lin, B. S. Zhang, M. K. Tseng, *Mater. Sci. Forum.* 331-337 (2000), p.1225.
- [11] R. L Bye, N. J. Kim, D. J. Skinner, D. Rayboud, A. M. Brown, *Allied-Signal Co.* (1987), p.283.
- [12] D. J. Skinner, R. L. Bye, D. Raybould, A. M. Brown, *Scr. Metall* 20 (1986), p.867.
- [13] V. R. V. Ramanan, D. J. Skinner, M. S. Zedalis, *Mater. Sci. Eng.* A134 (1991), p.912.
- [14] M. Cooper, K. Robinson, *Acta Cryst.* 20 (1966), p.614.
- [15] M. Cooper, *Acta Cryst.* 23 (1967), p.1106.